

145

The Design and Optimization of Complex NMR Experiments. Application to a Triple-Resonance Pulse Scheme Correlating $H\alpha$, NH, and ^{15}N Chemical Shifts in ^{15}N - ^{13}C -Labeled Proteins

LEWIS E. KAY, MITSUHIKO IKURA, AND AD BAX

Laboratory of Chemical Physics, Building 2, National Institute of Diabetes and Digestive and Kidney
Diseases, National Institutes of Health, Bethesda, Maryland 20892

Received August 17, 1990

Sequence-specific assignments of the backbone resonances of proteins form the basis for further study of the structural and dynamic properties of the molecule under investigation. Traditional assignment strategies have relied on through-bond and through-space connectivities provided by homonuclear COSY, HOHAHA/TOCSY, and NOESY spectra (1-4). While very fruitful for proteins less than 10 kDa, this approach becomes difficult for larger systems, due to extensive overlap and decreasing sensitivity of experiments relying on through-bond connectivities.

Recently, we have proposed a novel approach for the sequential assignment of 1H , ^{13}C , and ^{15}N spectra of larger proteins based on triple-resonance three-dimensional NMR spectroscopy (5, 6). These experiments exploit the relatively large one-bond J couplings between the backbone ^{13}C and ^{15}N nuclei and between the backbone protons and the ^{13}C and ^{15}N nuclei to which they are directly attached. Because the couplings are often large compared to pertinent linewidths for proteins less than 25 kDa in molecular weight, magnetization can be transferred between spins in an efficient manner, with the resultant spectra having good sensitivity. Moreover, because the experiments are recorded in the "3D mode," spectral overlap is virtually eliminated.

The sequential assignment of ^{13}C - ^{15}N -labeled proteins using the triple-resonance approach is aided considerably by the HOHAHA-HMQC experiment (7). For example, the HNCA triple-resonance experiment correlates the NH and ^{15}N chemical shifts with the intrasidue $C\alpha$ chemical shift. When combined with the HNCA experiment, the HOHAHA-HMQC experiment (which correlates ^{15}N , NH, and $H\alpha$ chemical shifts) firmly establishes intrasidue correlations between pairs of ^{15}N -NH and $C\alpha$ - $H\alpha$ backbone resonances, despite significant overlap in 1D 1H , ^{15}N , and ^{13}C spectra. Linking the ^{15}N , NH, $C\alpha$, and $H\alpha$ chemical shifts is the first step in the sequential assignment process using this new approach. Unlike the triple-resonance experiments, the HOHAHA-HMQC experiment is very sensitive to the secondary structure of the protein under study, as the efficiency of magnetization transfer between NH and $H\alpha$ protons depends strongly on the NH- $H\alpha$ scalar couplings. These couplings are, in turn, strongly related to the backbone angle ϕ and are less than 6 Hz in regions of regular α -helical secondary structure. For larger proteins rich in α -helical content, a substantial number of NH- $H\alpha$ connectivities are often found to be weak or missing. In this paper a triple-

resonance 3D NMR pulse scheme which provides NH-H α correlations in a manner completely independent of secondary structure is described and demonstrated. In particular, we describe how this experiment was optimized from the perspective of employing a minimal number of pulses and minimizing the time for magnetization dephasing and refocusing during coherence transfers. With the wide array of "pulse-sequence building blocks" available to the NMR spectroscopist it is relatively straightforward to design a new experiment which generates the desired correlations. For the more complex experiments frequently employed in higher-dimensionality NMR it becomes crucial, however, to construct pulse schemes which are as efficient as possible. As demonstrated here, frequently this is achieved in a straightforward fashion.

Figure 1a shows one possible 3D pulse scheme for correlating NH and H α chemical shifts. This experiment is based on the transfer of magnetization from H α to NH spins via successive through-bond transfers between the directly coupled H α -C α , C α -¹⁵N, and ¹⁵N-NH pairs and is thus termed H(CA)NNH. This scheme is essentially a generalization of a 2D HETERO-RELAY pulse sequence proposed by Montelione and Wagner (8). The sequence can be easily understood as follows. H α proton polarization is allowed to evolve for a time t_1 and subsequently transferred by an INEPT sequence (9) to the directly coupled C α spin. Immediately prior to the transfer a long proton pulse (several milliseconds) is applied to suppress the water signal (10). This is most easily achieved if the carrier is placed on the water resonance. In this method, the components of magnetization from the water and antiphase H α spins are orthogonal immediately prior to the water purge pulse. Following the purge pulse and the application of 90° ¹H and ¹³C α pulses (90° _{ϕ_3} and 90° _{ϕ_4} in Fig. 1), the antiphase C α polarization is allowed to refocus with respect to the H α spins during a period $2\tau_{II}$, after which C α -¹⁵N dephasing occurs during the interval $2\delta_{II}$. The following 90° ¹³C pulse creates carbon-nitrogen zz magnetization (S_zN_z , where S and N are carbon and nitrogen spins, respectively) and this is followed by an additional long proton pulse (9 ms) to further suppress the intense water resonance. Empirically, we have found that the application of a 90° pulse immediately following the long purge pulse helps to minimize residual signal from water. Subsequently magnetization is transferred to the nitrogen spin, and evolution proceeds during t_2 . The effects of ¹H-¹⁵N and ¹³C α -¹⁵N J coupling are removed by the application of ¹H and ¹³C 180° pulses at the midpoint of t_2 . After the t_2 evolution period, ¹⁵N magnetization is refocused with respect to the C α spin during the delay $2\delta_{III}$ and subsequently defocused with respect to the directly coupled NH proton during the period $2\tau_{III}$ to allow transfer of magnetization back to NH protons via an INEPT sequence. Amide protons are detected during t_3 with ¹⁵N decoupling. It should be noted that the effects of the one-bond C α -carbonyl (C') couplings are removed by a weak GARP decoupling field (11) applied in the middle of the C' resonances during the period when C α transverse magnetization evolves. This scheme generates a 3D data set which after Fourier transformation in all three dimensions, yields cross peaks at coordinates: $[\omega_1, \omega_2, \omega_3] = [H\alpha^i, {}^{15}N^i, NH^i]$ and $[\omega_1, \omega_2, \omega_3] = [H\alpha^{i-1}, {}^{15}N^i, NH^i]$. Note that there is a simultaneous transfer of magnetization from the C α spin of residues $i-1$ and i to the ¹⁵N spin of residue i due to the presence of both a direct (~ 11 Hz) and a two-bond (~ 7 Hz) C α -¹⁵N coupling.

In principle, the pulse scheme of Fig. 1a represents a feasible approach for providing NH-H α correlations. However, a closer inspection suggests that the rather large number

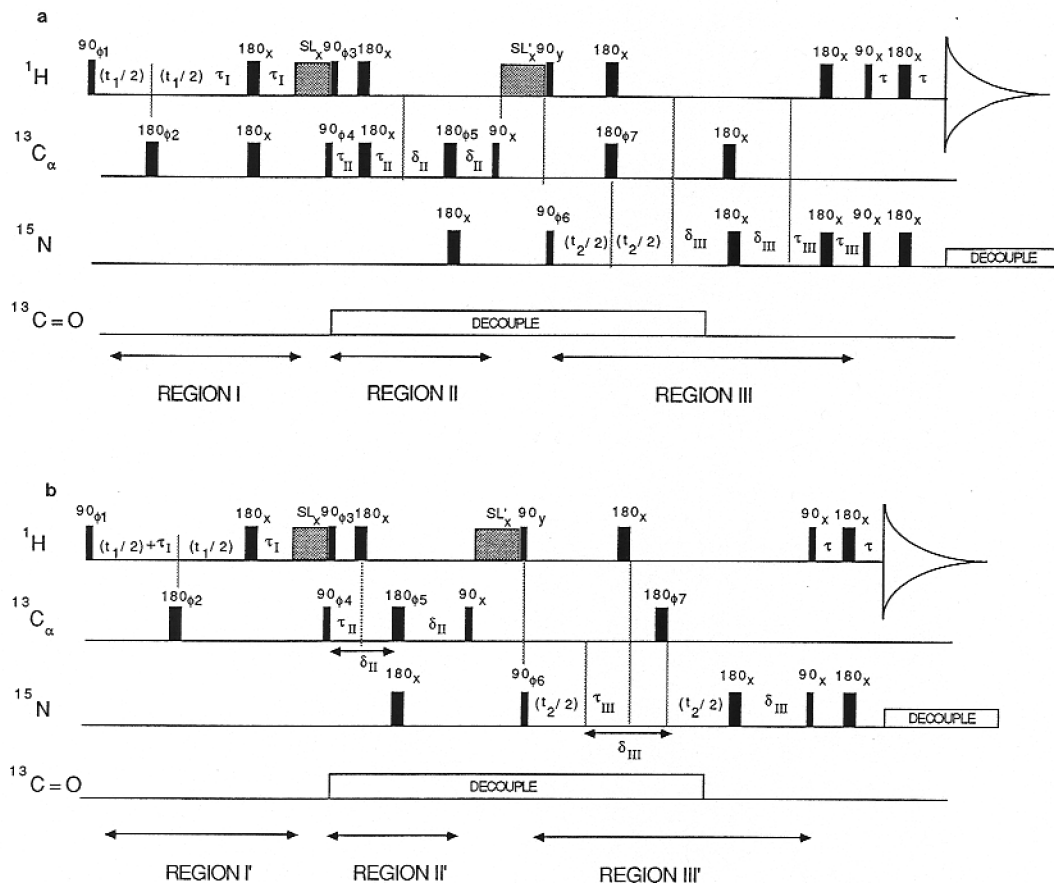


FIG. 1. Comparison of two different pulse schemes for the H(CA)NNH experiment. The sequence of (b) is obtained from (a) by concatenation of 180° pulses (17, 19, 20). In this way five 180° pulses were eliminated. Typical durations used are $\tau_I = 1.5$ ms, $\tau_{II} = 1.7$ ms, $\delta_{II} = 12.5$ ms, $\tau_{III} = 2.75$ ms, $\delta_{III} = 11.5$ ms, and $\tau = 2.25$ ms. This optimizes intraresidue transfer of magnetization for all residues except glycine (see Eq. [9]). For the case of glycine a value of $\tau_{II} \sim 0.8\text{--}0.9$ ms should be employed. Water suppression is achieved through the use of two purge pulses, SL_x and SL'_x , applied for 1.5 and 9 ms, respectively (10). The carrier is positioned on the water resonance. The phase-cycling scheme employed is as follows: $\phi_1 = x$; $\phi_2 = x, -x$; $\phi_3 = x, -x$; $\phi_4 = 2(x), 2(-x)$; $\phi_5 = 4(x), 4(y), 4(-x), 4(-y)$; $\phi_6 = 16(x), 16(-x)$; $\phi_7 = 8(x), 8(-x)$; Acq. = $2(x, -x - x, x, -x, x, x, -x), 2(-x, x, x, -x, x, -x, -x, x)$. The phases ϕ_1 and ϕ_6 are incremented independently by 90° to generate complex data in the t_1 and t_2 dimensions, respectively, using the States-TPPI method (21). The ^{15}N pulses and phases are generated by a homebuilt third channel described previously (6). Carbonyl decoupling is achieved with a GARP decoupling sequence (11) using a 500 Hz field. ^{15}N decoupling during acquisition is achieved using a 1 kHz RF field with the WALTZ decoupling sequence (22).

of π pulses in the sequence (six ^{13}C , four ^{15}N , and five ^1H π pulses) may result in a serious sensitivity loss because of finite RF field homogeneity. Moreover, the large number of pulses necessitates a lengthy phase cycling scheme in order to eliminate artifacts generated by pulse imperfections. Extensive phase cycling is usually not possible if three- or four-dimensional (12) NMR spectra are to be recorded in reasonable

amounts of time (t_3). Finally, for proteins it is crucial that the total duration of fixed delays needed for defocusing and refocusing transverse magnetization be minimized. As is shown below, both the number of 180° pulses and these durations can be shortened significantly by optimization of the pulse scheme.

A functionally equivalent version of the sequence of Fig. 1a which minimizes both the number of pulses and the total duration of delays needed for the $H\alpha$ to NH magnetization transfer is illustrated in Fig. 1b. The construction of this sequence can be rationalized by dividing the sequence of Fig. 1a into three independent parts (I, II, and III in Fig. 1a) and describing how each section can be simplified. The corresponding simplified versions of regions I, II, and III are indicated by I', II', and III' in the sequence of Fig. 1b. In the discussion that follows, we consider only the fate of magnetization that is retained by the phase-cycling scheme indicated in the legend to Fig. 1. This restricts our focus to the description of the evolution of $H\alpha$, $C\alpha$, and ^{15}N magnetization during regions I, II and III, respectively.

In region I transverse proton magnetization is required to evolve for a period t_1 and becomes antiphase with respect to the directly coupled $C\alpha$ spin during a delay of $2\tau_1$. As is discussed below, it is possible to simplify this portion of the sequence to

$$\begin{array}{c} {}^1\text{H: } A_1 \quad B_1 \quad \pi \quad C_1 \\ {}^{13}\text{C: } \quad \quad \pi \\ \quad \quad \quad \longleftrightarrow \\ \quad \quad \quad \text{REGION I}' \end{array}$$

where A_1 , B_1 , and C_1 are delays during which magnetization evolves. During this period only transverse ^1H magnetization is present and a straightforward calculation shows that ^1H magnetization evolves for a time of $A_1 + B_1 - C_1$ due to chemical shift and that the one-bond ^1H - ^{13}C coupling proceeds for a duration of $A_1 - B_1 + C_1$. Therefore, we require that

$$A_1 + B_1 - C_1 = t_1. \quad [1]$$

Denoting the time during which ^1H - ^{13}C scalar evolution proceeds as $2\tau_1$ gives

$$A_1 - B_1 + C_1 = 2\tau_1. \quad [2]$$

A solution to Eqs. [1] and [2] is

$$\begin{array}{l} A_1 = t_1/2 + \tau_1 \\ B_1 = t_1/2 \\ C_1 = \tau_1, \end{array} \quad [3]$$

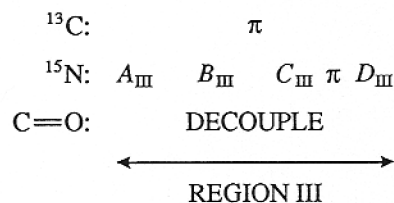
which is indicated in region I' of Fig. 1b. Note that this construct has resulted in the elimination of one $C\alpha$ 180° pulse relative to region I of Fig. 1a. This type of concatenation of 180° pulses during the evolution period can also be used to simplify a number of the older ^1H - ^{13}C shift correlation experiments (14-17).

where ${}^1J_{\text{CN}}$, ${}^2J_{\text{CN}}$, $J_{\text{C}\alpha\beta}$, J_{HC} are the coupling constants describing the one-bond $\text{C}\alpha$ - ${}^{15}\text{N}$, the two-bond $\text{C}\alpha$ - ${}^{15}\text{N}$, the $\text{C}\alpha$ - $\text{C}\beta$, and the ${}^1\text{H}\alpha$ - ${}^{13}\text{C}\alpha$ coupling interactions, respectively, and $T_{2\text{C}\alpha}$ is the $\text{C}\alpha$ transverse relaxation time. Since in this case $J_{\text{HC}} \gg J_{\text{CN}}$, Eq. [8] indicates that an optimal choice for $A_{\text{II}} = \tau_{\text{II}}$ is $1/(4J_{\text{HC}})$, independent of the transverse relaxation rate, $T_{2\text{C}\alpha}$. Optimal choices for $D_{\text{II}} = \delta_{\text{II}}$ and C_{II} are functions of $T_{2\text{C}\alpha}$ and all of the scalar couplings with the exception of J_{HC} . With $\{{}^1J_{\text{CN}}, {}^2J_{\text{CN}}, J_{\text{C}\alpha\beta}, 1/(\pi T_{2\text{C}\alpha})\} = (11, 7, 37, 15 \text{ Hz})$ the maximum of Eq. [8] is obtained with $C_{\text{II}} = 0$ and $\delta_{\text{II}} = D_{\text{II}} = 12.5 \text{ ms}$. As the linewidth increases, the value of D_{II} which optimizes Eq. [8] decreases slowly. For example, for a $\text{C}\alpha$ linewidth of 20 Hz, the values of C_{II} and D_{II} which give a maximum are 0 and 12 ms, respectively. Thus, for fully ${}^{13}\text{C}$ -enriched proteins in the 15–25 kDa molecular weight range, setting $C_{\text{II}} = 0$ and D_{II} to 12–13 ms will optimize transfer from $\text{C}\alpha$ to ${}^{15}\text{N}$ for the range of $\text{C}\alpha$ linewidths typically encountered. Finally, B_{II} is set to $D_{\text{II}} - A_{\text{II}}$ in the sequence of Fig. 1b to satisfy Eq. [4]. In a similar manner, the transfer function for the glycine intraresidue connectivities is given by

$$\sin(2\pi {}^1J_{\text{CN}}\delta_{\text{II}})\cos(2\pi {}^2J_{\text{CN}}\delta_{\text{II}})\sin(2\pi J_{\text{HC}}\tau_{\text{II}})\cos(2\pi J_{\text{HC}}\tau_{\text{II}})\exp\{-2(C_{\text{II}} + \delta_{\text{II}})/T_{2\text{C}\alpha}\}. \quad [9]$$

For this situation $A_{\text{II}} = \tau_{\text{II}} = 1/(8J_{\text{HC}})$ and $C_{\text{II}} = 0$ give optimal results, and with $\{{}^1J_{\text{CN}}, {}^2J_{\text{CN}}, 1/(\pi T_{2\text{C}\alpha})\} = (11, 7, 15 \text{ Hz})$ as before, a value of $\delta_{\text{II}} = D_{\text{II}} = 8.0 \text{ ms}$ should be chosen. In region II', the $\text{C}\alpha$ - $\text{H}\alpha$ refocusing period and the $\text{C}\alpha$ - ${}^{15}\text{N}$ defocusing period overlap, thus shortening the total duration required, in a manner similar to that in the case previously described for heteronuclear RELAY spectroscopy (17) and a number of 3D pulse schemes developed in our laboratory (19, 20). A comparison of regions II and II' indicates that in addition to shortening the total required duration, a $\text{C}\alpha$ 180° pulse has been eliminated.

Region III of Fig. 1a may be simplified as



where A_{III} , B_{III} , C_{III} , and D_{III} denote evolution periods. During this interval the time course of ${}^{15}\text{N}$ magnetization need only be considered. An operator description of the evolution of ${}^{15}\text{N}$ magnetization during this period indicates that ${}^{15}\text{N}$ chemical shift evolves for a time $A_{\text{III}} + B_{\text{III}} + C_{\text{III}} - D_{\text{III}}$, $\text{C}\alpha$ - ${}^{15}\text{N}$ J evolution proceeds during $A_{\text{III}} + B_{\text{III}} - C_{\text{III}} + D_{\text{III}}$, and ${}^1\text{H}$ - ${}^{15}\text{N}$ scalar coupling is operative during the interval $A_{\text{III}} - B_{\text{III}} - C_{\text{III}} + D_{\text{III}}$. We require that

$$A_{\text{III}} + B_{\text{III}} + C_{\text{III}} - D_{\text{III}} = t_2 \quad [10]$$

$$A_{\text{III}} + B_{\text{III}} - C_{\text{III}} + D_{\text{III}} = 2\delta_{\text{III}} \quad [11]$$

$$A_{\text{III}} - B_{\text{III}} - C_{\text{III}} + D_{\text{III}} = 2\tau_{\text{III}}, \quad [12]$$

where t_2 is the ^{15}N chemical-shift evolution time and $2\delta_{\text{III}}$ and $2\tau_{\text{III}}$ denote the times needed for ^{15}N evolution due to $\text{C}\alpha$ - ^{15}N and ^{15}N -NH scalar couplings, respectively. A solution to Eqs. [10]–[12] is obtained with

$$\begin{aligned} A_{\text{III}} &= t_2/2 + \tau_{\text{III}} \\ B_{\text{III}} &= \delta_{\text{III}} - \tau_{\text{III}} \\ C_{\text{III}} &= t_2/2 \\ D_{\text{III}} &= \delta_{\text{III}}. \end{aligned} \quad [13]$$

Optimal values for τ_{III} and δ_{III} are obtained by requiring that the transfer of magnetization from ^{15}N to the directly coupled NH spin be maximal. This requires optimization of a transfer function of the form

$$\sin(2\pi^1J_{\text{CN}}\delta_{\text{III}})\cos(2\pi^2J_{\text{CN}}\delta_{\text{III}})\sin(2\pi J_{\text{NH}}\tau_{\text{III}})\exp(-2\delta_{\text{III}}/T_{2\text{N}}), \quad [14]$$

where J_{NH} and $T_{2\text{N}}$ are the ^{15}N -NH scalar coupling constant and the ^{15}N transverse relaxation time, respectively, and $^1J_{\text{CN}}$ and $^2J_{\text{CN}}$ are defined as before. Equation [14] indicates that since $J_{\text{NH}} \gg J_{\text{CN}}$, τ_{III} should be set to $1/(4J_{\text{NH}})$, independent of $T_{2\text{N}}$, and for $\{^1J_{\text{CN}}, ^2J_{\text{CN}}, 1/(\pi T_{2\text{N}})\} = (11, 7, 7 \text{ Hz})$ a value for δ_{III} of 11.5 ms is optimal. The logic described above leads to a reduction of the number of 180° pulses in region III from 6 to 3. In addition, in region III' the total duration has been reduced by recognizing that the $\text{C}\alpha$ - ^{15}N refocusing period and the ^{15}N -NH defocusing period can proceed simultaneously.

Figure 2 illustrates typical slices taken from the H(CA)NNH 3D spectrum of uniformly ^{15}N - ^{13}C -labeled calmodulin (1.5 mM) complexed with a 26 amino-acid fragment of skeletal myosin light chain kinase in 95% $\text{H}_2\text{O}/5\% \text{D}_2\text{O}$, 100 mM KCl, 6 mM Ca^{2+} , pH 6.8, and recorded at 35°C . The pulse scheme of Fig. 1b was employed. The two slices at ^{15}N frequencies of 116.7 ppm (A) and 125.2 ppm (B) display intraresidue correlations between NH and $\text{H}\alpha$ resonances. In addition, weaker interresidue correlations are observed connecting the NH shift with the $\text{H}\alpha$ shift of the preceding residue. This provides valuable sequential connectivity information which, when combined with the results of other triple-resonance experiments (5, 6), enables the complete backbone assignment of ^{15}N - ^{13}C -labeled proteins to be made in a relatively straightforward manner.

In summary, we have described an approach which permits a dramatic reduction in the length of many complex pulse schemes by concatenation of pulses. For the triple-resonance sequence considered here the number of 180° refocusing pulses is decreased from 15 to 10. This dramatically improves the sensitivity of the resultant spectra by reducing the effects of RF inhomogeneity and pulse imperfections and in addition minimizes the phase-cycling schemes necessary to eliminate artifacts. Moreover, because refocusing and defocusing of scalar couplings are allowed to proceed simultaneously, the total time in which transverse magnetization evolves is decreased. For example, for the H(CA)NNH sequence, the refocusing of the $\text{C}\alpha$ magnetization due to the ^1H - ^{13}C coupling during $\text{C}\alpha$ evolution and the dephasing of the ^{15}N magnetization due to the ^{15}N -NH coupling during ^{15}N precession are obtained for "free."

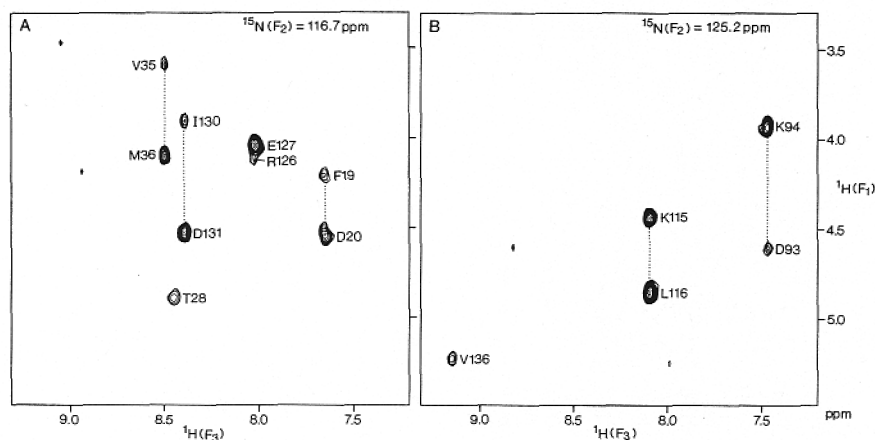


FIG. 2. Sections of (F_1 , F_3) slices of the H(CA)NNH 3D spectrum of 1.5 mM calmodulin complexed with a 26 amino-acid residue fragment of myosin light chain kinase recorded on a Bruker AM500 spectrometer. Spectra at ^{15}N frequencies of 116.7 ppm (A) and 125.2 ppm (B) are displayed. The spectra show intense intraresidue NH- $\text{H}\alpha$ correlations and weaker connectivities between the NH and the $\text{H}\alpha$ from the preceding residue. The 3D spectrum results from a (64 complex) \times (32 complex) \times (1K real) data matrix (8 megaword) with acquisition times of 29.4, 32, and 62 ms in t_1 , t_2 , and t_3 , respectively. The length of the t_2 time domain was doubled using linear prediction (23, 24). After zero-filling the digital resolution is 17 Hz (F_1 , $\text{H}\alpha$), 8 Hz (F_2 , ^{15}N), and 4 Hz (F_3 , NH). Because of the relatively short $\text{H}\alpha$ longitudinal relaxation time, a short (0.8 s) relaxation delay was used, resulting in a total measuring time of \sim 60 hours. A baseline correction in the t_3 time domain was used to reduce the intensity of the residual water signal (25). The spectrum was processed on a Sun Sparc Workstation using in-house routines for processing in F_2 (26), together with the commercially available software package NMR2 (New Methods Research, Inc., Syracuse, New York) for processing the F_1 - F_3 planes.

The approach described should have important implications for three- and four-dimensional NMR spectroscopy of larger proteins, where maximizing sensitivity and minimizing measuring times are critical.

ACKNOWLEDGMENTS

We thank Marie Krinks for preparation of the calmodulin sample. L.E.K. is the recipient of a Centennial Fellowship from the Medical Research Council of Canada. This research was supported by the AIDS Directed Anti-Viral Program of the Office of the Director of the National Institutes of Health.

REFERENCES

1. K. WÜTHRICH, "NMR of Proteins and Nucleic Acids," Wiley, New York, 1986.
2. G. M. CLORE AND A. M. GRONENBORN, *CRC Crit. Rev. Biochem. Biol.* **24**, 479 (1989).
3. A. BAX, *Annu. Rev. Biochem.* **58**, 223 (1989).
4. R. KAPTEIN, R. BOELEN, R. M. SCHEEK, AND W. F. VAN GUNSTEREN, *Biochemistry* **27**, 5389 (1988).
5. M. IKURA, L. E. KAY, AND A. BAX, *Biochemistry* **29**, 4659 (1990).
6. L. E. KAY, M. IKURA, R. TSCHUDIN, AND A. BAX, *J. Magn. Reson.*, **89**, 496 (1990).
7. D. MARION, P. C. DRISCOLL, L. E. KAY, P. T. WINGFIELD, A. BAX, A. M. GRONENBORN, AND G. M. CLORE, *Biochemistry* **28**, 6150 (1989).
8. G. T. MONTELEONE AND G. WAGNER, *J. Magn. Reson.* **87**, 183 (1990).
9. G. A. MORRIS AND R. FREEMAN, *J. Am. Chem. Soc.* **101**, 760 (1979).

10. B. A. MESSERLE, G. WIDER, G. OTTING, C. WEBER, AND K. WÜTHRICH, *J. Magn. Reson.* **85**, 608 (1989).
11. A. J. SHAKA, P. BARKER, AND R. FREEMAN, *J. Magn. Reson.* **53**, 313 (1983).
12. L. E. KAY, G. M. CLORE, A. BAX, AND A. M. GRONENBORN, *Science* **249**, 411 (1990).
13. A. BAX, G. M. CLORE, P. C. DRISCOLL, A. M. GRONENBORN, M. IKURA, AND L. E. KAY, *J. Magn. Reson.* **87**, 620 (1990).
14. R. R. ERNST, G. BODENHAUSEN, AND A. WOKAUN, "Principles of Nuclear Magnetic Resonance in One and Two Dimensions," p. 472, Fig. 8.5.3.c, Clarendon Press, Oxford, 1988.
15. L. D. FIELD AND B. A. MESSERLE, *J. Magn. Reson.* **62**, 453 (1985).
16. A. E. DEROME, "Modern NMR Techniques for Chemistry Research," p. 247, Fig. 9.2.c, Pergamon, Oxford, 1987.
17. A. BAX, *J. Magn. Reson.* **53**, 149 (1983).
18. R. R. ERNST, G. BODENHAUSEN, AND A. WOKAUN, "Principles of Nuclear Magnetic Resonance in One and Two Dimensions," Chap. 2, Clarendon Press, Oxford, 1988.
19. L. E. KAY, M. IKURA, AND A. BAX, *J. Am. Chem. Soc.* **112**, 888 (1990).
20. A. BAX, G. M. CLORE, AND A. M. GRONENBORN, *J. Magn. Reson.* **88**, 425 (1990).
21. D. MARION, M. IKURA, R. TSCHUDIN, AND A. BAX, *J. Magn. Reson.* **85**, 393 (1989).
22. A. J. SHAKA, J. KEELER, T. FRENKIEL, AND R. FREEMAN, *J. Magn. Reson.* **52**, 334 (1983).
23. H. BARKHUISEN, R. DE BEER, W. M. M. J. BOVEE, AND D. VAN ORMONDT, *J. Magn. Reson.* **61**, 465 (1985).
24. A. E. SCHUSSHEIM AND D. COWBURN, *J. Magn. Reson.* **71**, 371 (1987).
25. D. MARION, M. IKURA, AND A. BAX, *J. Magn. Reson.* **84**, 425 (1989).
26. L. E. KAY, D. MARION, AND A. BAX, *J. Magn. Reson.* **84**, 72 (1989).